PERGAMON

Polyhedron 20 (2001) 1599–1606

POLYHEDRON

www.elsevier.nl/locate/poly

Quasi-static nature of the light induced thermal hysteresis in $[Fe(ptz)_6](BF_4)_2$ spin-transition solid

Jelena Jeftić [a,*], Marie Matsarski [b], Andreas Hauser [b], Antoine Goujon [c], Epiphane Codjovi [c], Jorge Linarès [c], François Varret [c]

[a] *ENSC Rennes, Avenue du Général Leclerc, Campus de Beaulieu, 35700 Rennes, France*
[b] *Université de Genève, Sciences II, 30 quai Ernest-Ansermet, 1211 Geneva 4, Switzerland*
[c] *Université de Versailles, LMOV, 45 Av. des Etats-Unis, 78035 Versailles Cedex, France*

Received 17 September 2000; accepted 6 December 2000

Abstract

The quasi-static nature of a light induced thermal hysteresis was studied on the spin-transition compound $[Fe(ptz)_6](BF_4)_2$, by means of optical spectroscopy and magnetic measurements in the temperature interval between 10 and 80 K. Various experimental procedures are discussed in relation to the competition between the two processes considered, namely the photoexitation and the high-spin → low-spin relaxation. A detailed discussion of the experimental parameters, which should be considered in order to avoid erroneous interpretations of LITH, is given. © 2001 Elsevier Science Ltd. All rights reserved.

Keywords: Light induced thermal hysteresis; $[Fe(ptz)_6](BF_4)_2$; Spin-transition solid

1. Introduction

$[Fe(ptz)_6](BF_4)_2$ is a spin-transition solid that was first synthesized in 1982 [1]. Ever since, this compound has been used as a model system for solid-state physical and photophysical investigations [2], in particular from a crystallographic point of view [3].

The title compound undergoes an abrupt spin transition, from the high-spin state ($^5T_2$) at elevated temperatures to the low-spin state ($^1A_1$) at low temperatures, with a hysteresis of $T_c^{\downarrow} = 128$ K and $T_c^{\uparrow} = 135$ K. The abruptness of the spin transition comes from cooperative effects of elastic origin [4]. Elastic interactions are related to the important difference in volume between the two spin states ($\Delta V_{HL} \approx 5\%$) [5]. The hysteresis itself originates from a coupling between the spin transition and a crystallographic phase transition [5,6].

A fascinating photophysical phenomenon discovered in the title complex is the LIESST effect (light induced excited spin state trapping) [7]. It comprises the conversion at low temperatures of the entire crystal from its low-spin ground state to the metastable high-spin state using photoexcitation by blue or green laser light. The self-accelerating nature of the high-spin → low-spin relaxation following such an excitation is a direct consequence of the cooperative effects, and serves to explain the origin of the light induced thermal hysteresis studied in this work.

The term "light induced thermal hysteresis" (LITH) was, in fact, introduced by Letard et al. [8], following the observation of a hysteresis loop for a mononuclear iron(II) derivative upon temperature scanning under permanent irradiation. For this compound the LIESST is incomplete at 20 K, with around 30% of the high-spin population, which makes a quantitative interpretation of LITH in this case quite difficult. Varret et al. explored the LITH behavior in $[Fe_xCo_{1-x}(btr)_2(NCS)_x \cdot H_2O]$ compound, where the LIESST effect is quantitative at 20 K, and the population of the metastable high-spin state is achieved to 100% [9]. Raising the temperature results in an accelerated kinetics of the high-spin → low-spin relaxation and thus a depopulation of the metastable high-spin state [10]. Under permanent irradiation the competition with relaxation may result in a quasi-static population of the

* Corresponding author. Tel.: +33-2-99871335; fax: +33-2-99871398.
E-mail address: jelena.jeftic@ensc-rennes.fr (J. Jeftić).

PII: S0277-5387(01)00660-X

metastable high-spin state. Varret et al. [9] further showed that in analogy to a hysteresis in the thermal spin transition, the LITH is also due to cooperative effects. They describe the interaction of the two processes (photoexitation and relaxation) using the macroscopic master equation. In addition, the term of "light induced optical hysteresis" (LIOH) is introduced. LIOH is obtained by variation of light intensities at a given temperature. Theoretical treatment of these phenomena has been given in Ref. [11]. The current studies of light phenomena coupled with other processes are oriented towards "light induced pressure hysteresis" (LIPH), for which the varying parameter is pressure [12].

In this work, we show the influence of experimental conditions, such as temperature scanning speed, irradiation wavelength and intensity of light used for LIESST, on the shape and nature of LITH.

2. Experimental

2.1. Sample preparation

The title compound, $[Fe(ptz)_6](BF_4)_2$, was first synthesized by Franke et al. [1]. We studied it in the form of single crystals of high optical quality. Crystals of small size ($0.1 \times 1 \times 2$ mm^3 or smaller) were used in order to avoid misleading effects due to unwanted high-spin/low-spin gradients that can be produced during photoexcitation in thicker crystals.

Upon slow cooling, the crystal undergoes a crystallographic phase transition from the rhombohedric to the triclinic phase at $T_c^{\downarrow} = 128$ K and $T_c^{\uparrow} = 135$ K [5,6,10]. To study the behavior in the rhombohedric phase, we quenched it by rapid cooling (from 200 to 50 K in less than 3 min).

2.2. Experimental techniques

We have used two experimental techniques for LITH experiments, namely *magnetic measurements* on the SQUID magnetometer (University of Versailles) and *absorption spectroscopy measurements* (University of Geneva). For magnetic measurements we take advantage of the important difference in magnetic moments between the low-spin ($S = 0$) and the high-spin ($S = 2$) state in the Fe(II) title compound. Optical measurements are based on the marked difference in colors between the two spin states. One can distinguish easily the low-spin state that has two intense d–d absorptions in the visible region of the spectrum, and is therefore red, from the high-spin state that absorbs in the infrared region and is colorless [7].

2.3. Optical measurements

Optical measurements were performed on single crystals placed on the cryostat sample holder, and cooled down to 10 K in a He(g) atmosphere. LIESST was performed with laser irradiation of ~ 1 mW mm^{-2} intensity at the wavelength of 453 nm from the Ar^+ laser (Spectra Physics). To detect the signal, we used a monochromator, a photon multiplier (Hamamatsu R928) and the Lock-in-Amplifier.

For each measured $n_{HS}(T)$ in the quasi-static LITH loop, several waiting hours were spent to establish the equilibrium between the photoexcitation and the relaxation.

The crystal is rapidly cooled down from the room temperature to 10 K and quenched in its $R3i$ crystallographic phase (high-temperature phase) [2,3]. At 10 K it is completely in the low-spin state. By the photoexcitation with the blue (or green) light, the LIESST process takes place and after certain time the crystal converts to a 100% metastable high-spin state [7].

2.4. Magnetic measurements in a SQUID magnetometer

A chosen crystal was placed on a plastic support in a SQUID magnetometer equipped with an optical fiber [13]. It was cooled down rapidly, from 200 to 50 K in less than 3 min, in order to quench the rhombohedric (high-temperature) crystallographic phase [2,5]. The magnetic signal was optimized at 10 K. Temperature dependent scanning measurements were performed. The magnetic susceptibility recorded was corrected for diamagnetic and paramagnetic contributions of the sample holder. The units for χT are (emu Oe^{-1} K), which represents the direct response from the SQUID magnetometer, without a correction to obtain the molar susceptibility, χ_m.

As a light source we used a 100 W Halogen lamp, where we added optical filters of the broad-band type.

2.4.1. Temperature scanning velocity

To check the scanning velocity effect on the LITH in crystals of $[Fe(ptz)_6](BF_4)_2$, scanning speed was set to 0.032 and 0.02 K min^{-1}, in the temperature range from 40 to 80 K. The total time needed to complete the LITH was about two or three days, respectively. In both series of measurements the scanning speed used between 10 and 40 K was the same, 1 K min^{-1}.

2.4.2. Intensity of the light upon photoexcitation

We used three voltage settings of a halogen lamp 11, 8 and 6.5 V. These values provide intensities of approximately 50, 40 and 30 mW cm^{-2} on the sample for the filter of 550 ± 50 nm and around 30% less for the filter of 450 ± 50 nm. Intensity was measured ex situ by a homemade bolometer.

2.4.3. Effect of the wavelength used for LIESST

We used broad-band filters, notably 450 ± 50 and 550 ± 50 nm. For the former value, the absorption takes place at the edge of the low-spin absorption band. In contrast, the 550 nm corresponds to the maximum value of the absorption band of the low-spin state. This has a consequence that the low-spin → high-spin photopopulation by blue light is more gradual than by green light. The crystal suffers minimally from the elastic constraints and usually does not break under blue light irradiation of moderate intensity.

3. Results and discussion

In Fig. 1, we see the magnetic susceptibility as a function of time for five different stages of one experiment. We use the fact that the magnetic susceptibility is proportional to the high-spin state which is paramagnetic ($S_{HS} = 2$) while χ has a constant value for the low-spin state which has the magnetic moment zero ($S_{HS} = 0$). Thus by the magnetic measurements in the SQUID magnetometer we can distinguish the two spin states and their proportion in the crystal at each time. We converted the original data using Curie law ($\chi \sim 1/T$) and corrected for the magnetic contribution of the sample holder that we measured separately. The magnetic unit used in the figures for χT are (emu Oe^{-1} K).

The first process recorded is LIESST represented by a photoexcitation curve (A). The form of the photoexcitation curve is rather non-cooperative and it takes around 2 h to completely convert the crystal from the low-spin to the high-spin state with the blue light of around 30 mW cm^{-2} intensity. The mechanism of the LIESST process at low temperatures (≈ 20 K) has been studied in detail by Hauser [14] as well as the mechanism of the self-acceleration of the high-spin → low-spin relaxation [15]. The second curve (B) of Fig. 1 represents the situation in which the LIESST and the relaxation are put in competition, at 53 K, and after a certain time give a steady state. The steady state results from comparable kinetic times of the LIESST process at 53 K and the relaxation process at the same temperature. Here, we can talk about a dynamical equilibrium which is established after around an hour for LIESST (pumping low-spin → high-spin) and relaxation (depopulation high-spin → low-spin).

The third curve (C) in Fig. 1 is the high-spin → low-spin relaxation in absence of light. The relaxation is highly cooperative with the acceleration factor $\alpha = 5$, where Eq. (1) holds [16]

$$k_{HL}(n_{LS},T) = k_{HL}(n_{LS} = 0,T)\exp(\alpha n_{LS}) \quad (1)$$

The mechanism of the relaxation is described as a non-adiabatic multiphonon process [17] in the strong coupling limit. Concerning the temperature influence on

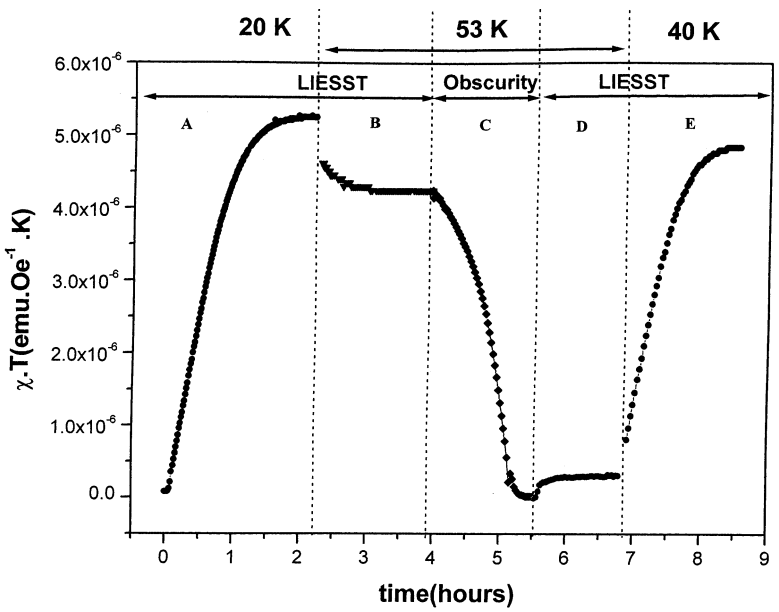

Fig. 1. Five (χT) curves as a function of time are shown either under continuous irradiation or in the darkness: (A) At 20 K the relaxation is very slow, thus the photoexcitation results in an almost complete population of the high-spin state. Under continuous irradiation the competition between LIESST and high-spin → low-spin relaxation results in a steady state after a sufficiently long time. (B) Upon raising the temperature to 53 K, the high-spin → low-spin relaxation becomes more rapid and the high-spin fraction in the steady state drops to $\sim 80\%$. (C) When the light source is turned off, the self-accelerated relaxation takes place and the crystal returns to 100% low-spin. (D) When the light is switched on again, keeping the temperature at 53 K, a different steady state from the above case is achieved. This is an indication of the presence of the LITH loop at this temperature. (E) At 40 K the relaxation is very slow and therefore the LIESST is a dominant process, resulting in almost quantitative population of the metastable high-spin state.

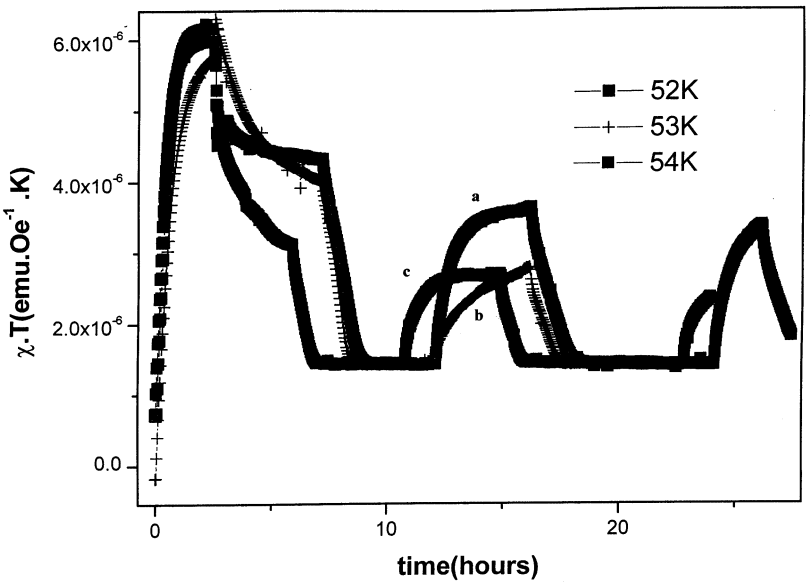

Fig. 2. The first four processes shown in Fig. 1(A)–(D) are compared for the $[Fe(ptz)_6](BF_4)_2$ crystal at 52, 53 and 54 K. The steady state HS fraction decreases with increasing temperature because the relaxation to the low-spin state becomes faster. At 52 K the steady state contains a high proportion of the high-spin state, compared to 54 K, where the relaxation is more rapid, and the high-spin state is present in smaller proportion.

the relaxation, we distinguish three regions in the Arrhenius diagram ($\ln k_{HL}$ vs. $1/T$): the tunneling region which expands from low temperatures up to around 40 K for the title compound and the thermally activated region above around 70 K with the linear dependence in the Arrhenius plot; the region between 40 and 70 K with the linear dependence in the Arrhenius plot; the region between 40 and 70 K shows an intermediate behavior.

In the fourth curve (D) of Fig. 1 we observe a progressive formation of another steady state, starting from 100% low-spin population, different from the first obtained steady state (B) at 53 K starting from 100% high-spin. The two different steady states (B and D) are the basis of an explanation of the formation of the LITH loop for one chosen temperature (here 53 K). Two different HS/LS proportions are formed under permanent irradiation, depending on whether the measurement started at 100% HS or at 100% LS, which results from cooperativity.

The fifth curve (E) in Fig. 1 is a photoexcitation curve at 40 K continuing the steady state. At 40 K the relaxation is quite slow and therefore the LIESST to the metastable HS state is almost complete.

In Fig. 2, we see the same experimental procedure as in Fig. 1, but this time for the mixture of crystallographic phases in the crystal of the title compounds $P1i$ and $R3i$. The mixture of the crystallographic phases occurs for kinetic reasons. The cooling of the crystal was not rapid enough to preserve it in the rhombohedric phase, nor slow enough to induce a complete phase transition to the triclinic phase. Three different experiments occur at temperatures of (a) 52, (b) 53 and (c) 54 K.

We observe the lack of cooperativity in relaxation, coming from almost non-cooperative relaxation in the triclinic phase [18]. The formation of steady states is a combination of two different relaxation kinetics in two different crystallographic phases, too. Further, at 52 K the steady state contains a high proportion of the high-spin state, compared to 54 K, where the relaxation is more rapid, and the high-spin state is present in smaller proportion.

From the less sigmoidal shape of the relaxation curves, we conclude that in addition to the $R3i$ crystallographic phase the $P1i$ phase is also present. This further means that the treatment of two different kinetics with $\alpha(R3i) = 5$ and $\alpha(P1i) = 1$ [10,18]. Without knowing the proportion of the two phases the quantitative interpretation of the curves here is not possible.

Fig. 3 represents a comparison between the slow temperature scanning experiment by light and obscurity on the diluted derivative of the title compound, namely $[Zn_{1-x}Fe_x(ptz)_6](BF_4)_2$ where $x = 0.1$. The crystal has been irradiated with a white halogen lamp, during the decrease in temperature from 295 to 20 K. The overlap with the spin-transition curve, measured in absence of light in the 12% iron derivative is perfect down to 75 K. Below 75 K down to 50 K we observe the predominant LIESST process and the diluted compound gets completely converted to the high-spin state. The temperature cycling back to room temperature gives a perfect overlap with the cooling curve and no hysteresis is present. This experiment has been performed for the high-temperature crystallographic phase of the diluted iron(II) compound, to stress the importance of cooperativity in forming LITH loops.

In Fig. 4, we show quasi-static LITH loops, recorded by the absorption spectroscopy. Fig. 4(a) shows the absorption spectra for (a) the high-temperature ($R3i$) and (b) the low-temperature ($P1i$) crystallographic phases of the title compound. The absorption spectra were collected for steady states starting from the 100% HS and the 100% LS, respectively. After several hours waiting at one temperature, with a constant photoexcitation intensity indicated in the figure, the hysteresis is not broader than 1.5 K for the $R3i$ phase and it is absent for the $P1i$ phase. This difference is explained on the basis of different cooperativities in the two phases: $\alpha(R3i) = 5$ while $\alpha(P1i) \approx 1$ [18].

Transition curves under permanent irradiation for the two crystallographic phases that approach the quasi-static LITH are shown in Fig. 4(c) and (d). Again, the LITH loop is present for the cooperative $R3i$ phase, while for the $P1i$ phase it does not show, within the experimental error.

Further experiment, shown in Fig. 5, gives an idea of the influence of the scanning speed on the LITH loop appearance. Most experimental cases of LITH published until now are in fact dynamical LITH loops, because even if one sets a very slow scanning speed the equilibrium is not necessarily achieved. This has been theoretically stressed out for the general case using the macroscopic approach by Varret et al. [11] and by analytical calculations by Hauser and Linares [19]. In Fig. 5, we compare two dynamic LITH loops by performing very slow scanning of the temperature, notably 0.032 and 0.02 K min^{-1} between 40 and 70 K. For these two different scanning speeds we observe a decrease in the width of the hysteresis of around 1 K. We define the hysteresis width as:

$$T_{1/2} = T_{1/2}(\text{ascending branch}) - T_{1/2}(\text{descending branch})$$

In the first case $\Delta T_{1/2}$ is 5 K, and in the second one 4 K. Thus, we see that we approach the quasi-static hysteresis by slow scanning, as expected.

Fig. 6 gives us an idea of the influence of light intensity and Fig. 7 the influence of the light wavelength on the shape of the LITH loop. The influence of the change in the photoexcitation wavelength from 450 to 550 nm results in a LITH shift towards higher temperatures for about 3 K, for the same lamp intensity. Decreasing the lamp intensity to 8 V (~ 40 mW cm^{-2}) brings the "450-nm induced" LITH and the "550-nm induced" LITH gets deformed, probably due to partial crystallographic phase transition or to HS–LS gradients in crystal formed by green light. On the other hand, we observe a completely deformed descending branch for LITH if the intensity of the photoexcitation is not high enough. Thus, for the curve at 6.5 V (< 30 mW cm^{-2}) lamp intensity we observe a photopopulation of around 80% HS which remains constant down to 10 K. The theoretical background for this experience was given in the Ref. [11].

4. Conclusions

We conclude that the quasi-statistic LITH is closely related to relatively high cooperativity of the title compound in the $R3i$ crystallographic phase ($\alpha = 5{,}14$). For the other crystallographic phase, $P1i$, the LITH loop is not observed. A study of the crystallographic phase transition under permanent irradiation will be given in another Ref. [6].

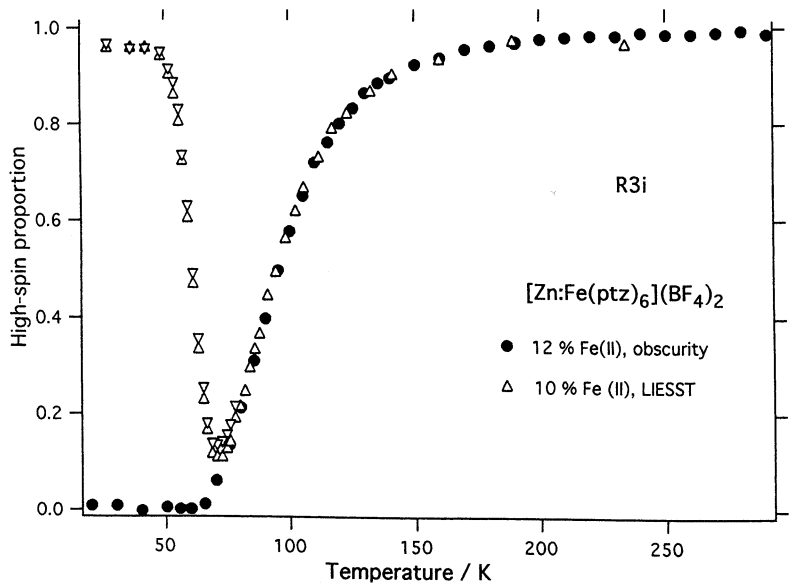

Fig. 3. Comparison of the thermal transition and the continuous irradiation curves for magnetically diluted $[Zn_{0.9}Fe_{0.1}(ptz)_6](BF_4)_2$. Around 75 K the reversible irradiation curve is obtained by decreasing and by increasing the temperature, this time without a LITH loop since no cooperative effects are present.

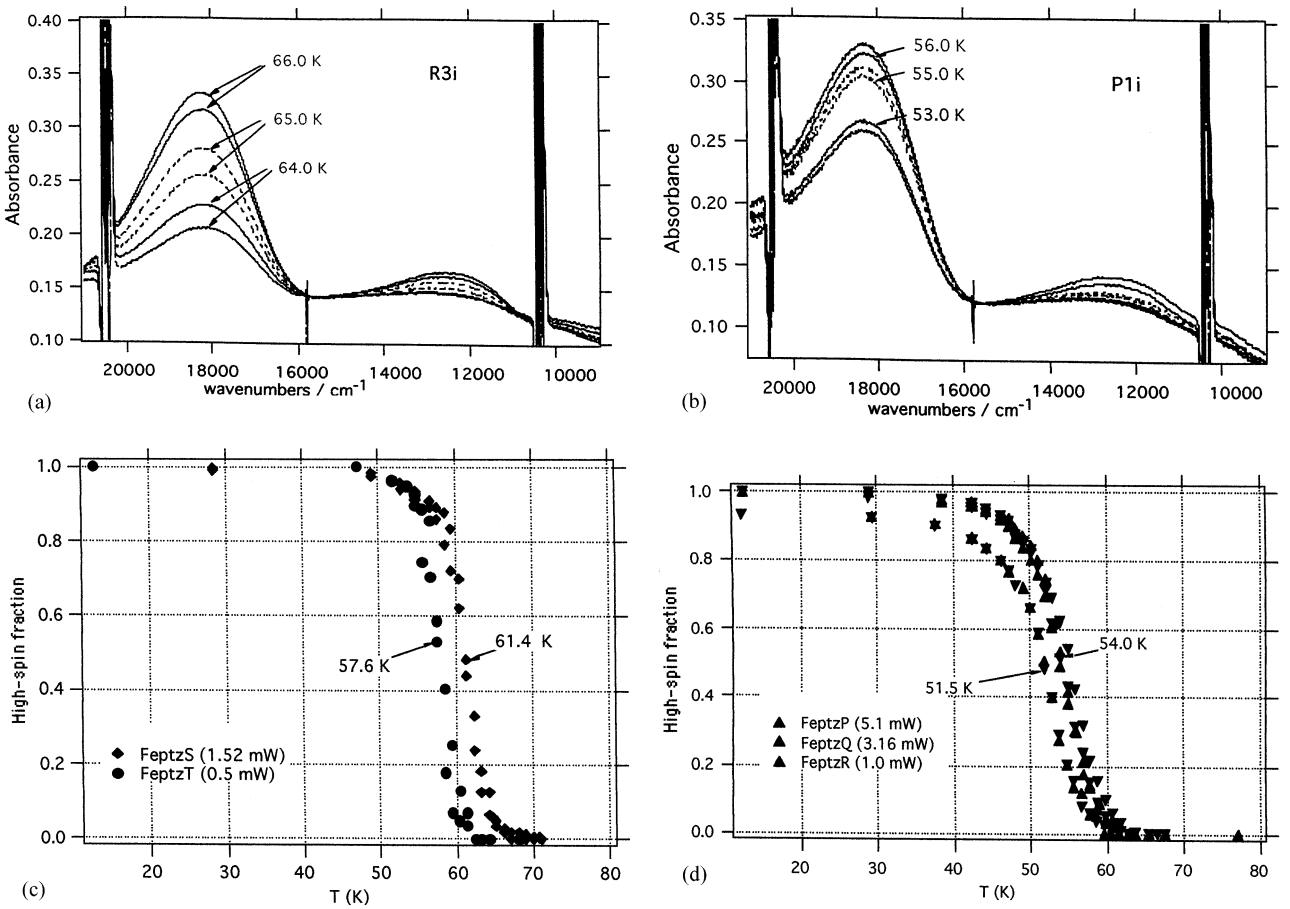

Fig. 4. (a) Full absorption spectra of the $[Fe(ptz)_6](BF_4)_2$ crystal in the crystallographic phase *R*3*i* show the presence of two different steady states obtained by starting from 100% LS or 100% HS, respectively. A clear evidence for LITH. (b) In the *P*1*i* phase no LITH is observed — the absorption spectra overlap within the experimental error. Lower measuring temperatures are taken because the relaxation in the *P*1*i* phase is too fast for this type of experiments at higher temperatures. (c) Full steady state curves obtained from absorption spectroscopy measurements. At each point (temperature) several hours were spent to be sure of the achieved steady state. For the *R*3*i* crystallographic phase of the $[Fe(ptz)_6](BF_4)_2$ crystal the LITH is 1.5 K wide. (d) Full steady state curves for the crystal in *P*1*i* phase. No LITH is observed, due to the reduced cooperativity for the relaxation in this phase.

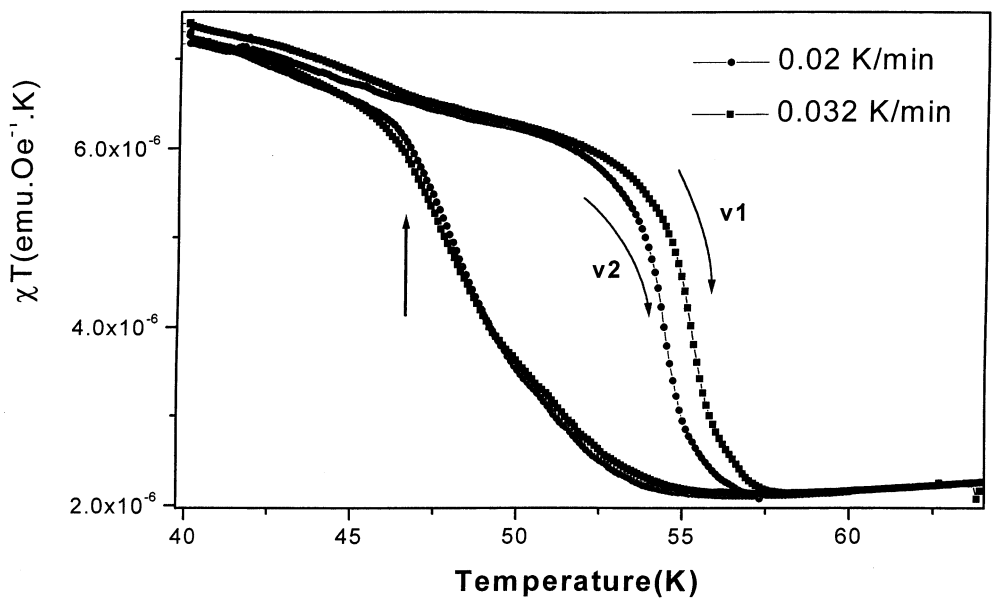

Fig. 5. The magnetic susceptibility as a function of temperature is measured at two different temperature scan rates: 0.02 and 0.032 K min^{-1}. The two resulting dynamic LITH loops differ in width (at $T_{1/2}$) by 1 K.

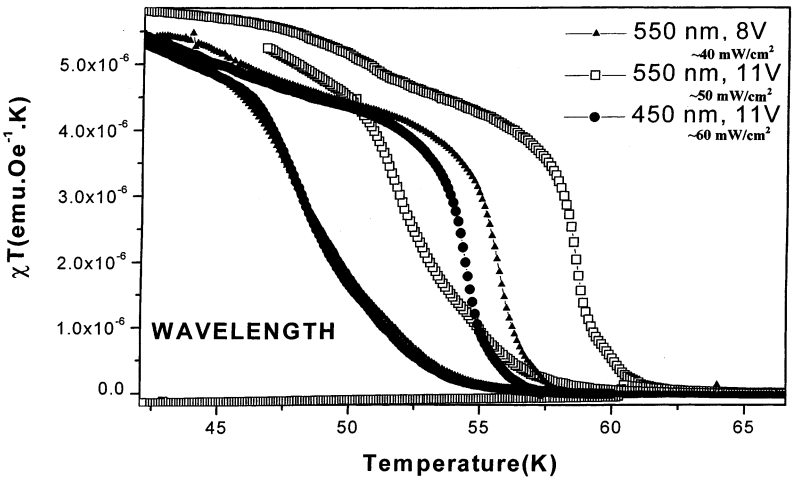

Fig. 6. The influence of different light wavelengths on the dynamical LITH. With 550 nm the dynamical LITH is shifted towards higher temperatures by 4 K, as compared to irradiation at 450 nm, because the green light is more efficient for the LIESST than the blue one.

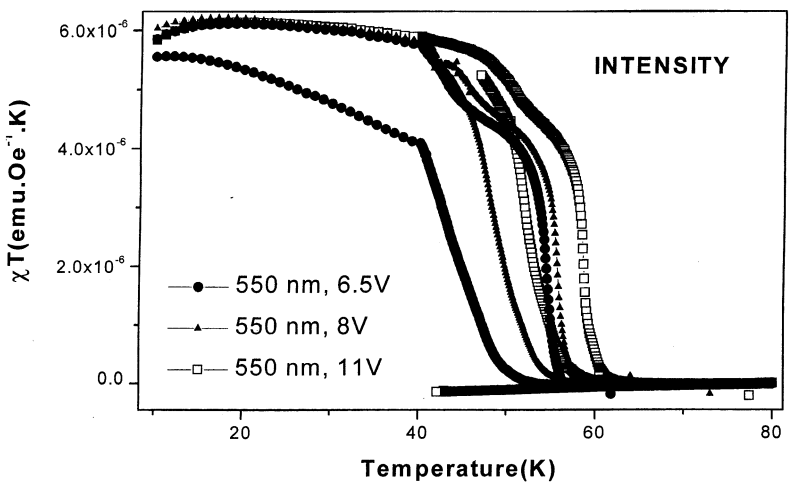

Fig. 7. Influence of different intensities on dynamic LITH loops. Higher intensity shifts an LITH loop towards higher temperatures. If the intensity is too low, LITH gets deformed because the LIESST is incomplete. For the descending branch in temperature we observe that the LITH loop remains opened and only around 80% of the high-spin state is continuously formed in the tunneling regime (below 40 K).

The experimental conditions to be followed in order to be sure of the origin of an eventual LITH loop are the following:

1. Quasi-static LITH means that the steady state between two processes (LIESST and relaxation) is achieved. This may imply very slow scanning of the temperature. Otherwise, we deal with a dynamic hysteresis.
2. The investigated crystal should be as thin as possible in order not to produce high-spin/low-spin gradients, which may lead to an apparent hysteresis.
3. The intensity of light should be kept low in order to avoid heating of the sample or the degradation of the quality of the crystal.
4. The crystal should remain in the same crystallographic phase during one measurement cycle, because of the very different relaxation kinetics in two phases, which may drastically influence the shape of the expected hysteresis.

The discussion of these aspects is based on variable temperature magnetic susceptibility and absorption spectroscopy measurements.

Acknowledgements

We thank H. Spiering, H. Cailleau, C. Ecolivet and M. Noguès for discussions and experimental help. The financial support of TMR-TOSS, SNSF, CNRS, BBW and ESF is gratefully acknowledged.

References

[1] P.L. Franke, J.G. Haasnoot, A.P. Zuur, Inorg. Chim. Acta 59 (1982) 5.
[2] P. Gütlich, A. Hauser, H. Spiering, Angew. Chem. 106 (1994) 2109.
[3] L. Wiehl, Acta Crystallogr., Sect. B 49 (1993) 289.
[4] H. Spiering, N. Willenbacher, J. Phys.: Condens. Matter 1 (1989) 10 089.
[5] J. Jeftić, H. Romstedt, A. Hauser, J. Phys. Chem. Solids 57 (1996) 1743.
[6] J. Jeftić, C. Ecolivet, A. Hauser, L. Bourgeois, M. Bertault, Solid State Commun., submitted for publication.
[7] S. Decurtins, P. Gütlich, K.M. Hasselbach, H. Spiering, A. Hauser, Inorg. Chem. 24 (1985) 2174.
[8] J.F. Letard, P. Guionneau, L. Rabardel, J.A.K. Howard, A.E. Goeta, D. Chasseau, O. Kahn, Inorg. Chem. 37 (1998) 4432.
[9] A. Desaix, O. Roubeau, J. Jeftić, J.G. Haasnoot, K. Boukheddaden, E. Codjovi, J. Linarès, M. Noguès, F. Varret, Eur. Phys. J. B 6 (1998) 183.
[10] A. Hauser, Comments Inorg. Chem. 17 (1995) 17.
[11] F. Varret, K. Boukheddaden, J. Jeftić, O. Roubeau, J. Mol. Cryst. Liq. Cryst. 335 (1999) 561.
[12] N. Menendez et al., TMR-TOSS Meeting, 1999; E. Codjovi et al., ICMM 2000 Conference, submitted for publication.
[13] E. Codjovi, W. Morscheidt, J. Jeftić, J. Linares, H. Constant-Machado, A. Desaix, F. Varret, J. Mol. Cryst. Liq. Cryst. 335 (1999) 583.
[14] A. Hauser, J. Chem. Phys. 94 (1991) 2741.
[15] A. Hauser, J. Jeftić, H. Romstedt, R. Hinek, H. Spiering, Coord. Chem. Rev. 190–192 (1999) 471.
[16] A. Hauser, Chem. Phys. Lett. 192 (1992) 65.
[17] A. Hauser, Comments Inorg. Chem. 17 (1995) 17; E. Bukhs, G. Navon, M. Bixon, J. Jortner, J. Am. Chem. Soc. 102 (1980) 2918.
[18] J. Jeftić, A. Hauser, J. Phys. Chem. B 101 (1997) 10 262.
[19] A. Hauser, J. Linares, unpublished results.